

# Satellite cell ablation attenuates short-term fast-to-slow fibre type transformations in rat fast-twitch skeletal muscle

Karen J. B. Martins · Gordon K. Murdoch · Yang Shu ·  
R. Luke W. Harris · Maria Gallo · Walter T. Dixon ·  
George R. Foxcroft · Tessa Gordon · Charles T. Putman

Received: 28 August 2008 / Accepted: 3 December 2008 / Published online: 8 January 2009  
© Springer-Verlag 2009

**Abstract** The purpose of this time-course study was to determine whether satellite cell ablation within rat tibialis anterior (TA) muscles exposed to short-term chronic low-frequency stimulation (CLFS) would limit fast-to-slow fibre type transformations. Satellite cells of the left TA were ablated by exposure to  $\gamma$ -irradiation before 1, 2, 5 or 10 days of CLFS and 1 week later where required. Control groups received only CLFS or a sham operation. Continuous infusion of 5-bromo-2'-deoxyuridine revealed that CLFS first induced an increase in satellite cell proliferation at 1 day, up to a maximum at 10 days over control (mean  $\pm$  SEM,  $5.7 \pm 0.7$  and  $20.4 \pm 1.0$  versus  $1.5 \pm 0.2$  mm<sup>-2</sup>, respectively,  $P < 0.007$ ) that was abolished by  $\gamma$ -irradiation.

Myosin heavy chain mRNA, immunohistochemical and sodium dodecyl sulfate polyacrylamide gel electrophoresis analyses revealed CLFS-induced fast-to-slow fibre type transformation began at 5 days and continued at 10 days; in those muscles that were also exposed to  $\gamma$ -irradiation, attenuation occurred within the fast fibre population, and the final fast-twitch to slow-twitch adaptation did not occur. These findings indicate satellite cells play active and obligatory roles early on in the time course during skeletal muscle fibre type adaptations to CLFS.

**Keywords** CLFS · Tibialis anterior · Immunohistochemistry · SDS-PAGE · Real-time RT-PCR · BrdU

K. J. B. Martins · Y. Shu · R. L. W. Harris · M. Gallo ·  
C. T. Putman  
Exercise Biochemistry Laboratory,  
Faculty of Physical Education and Recreation,  
University of Alberta,  
Edmonton, AB, Canada T6G 2H9

G. K. Murdoch · W. T. Dixon · G. R. Foxcroft  
Department of Agricultural, Food and Nutritional Sciences,  
University of Alberta,  
Edmonton, AB, Canada T6G 2P5

T. Gordon  
Division of Physical Medicine and Rehabilitation,  
University of Alberta,  
Edmonton, AB, Canada T6G 2S2

R. L. W. Harris · T. Gordon · C. T. Putman  
The Centre for Neuroscience, Faculty of Medicine and Dentistry,  
University of Alberta,  
Edmonton, AB, Canada T6G 2S2

C. T. Putman (✉)  
E-417 Van Vliet Centre, University of Alberta,  
Edmonton, Alberta, Canada T6G 2H9  
e-mail: tputman@ualberta.ca

## Introduction

Adult skeletal muscle contains heterogeneous, post-mitotic fibres that are capable of adjusting their structural, functional, metabolic and molecular properties in response to altered contractile demands such as endurance exercise. Myosin heavy chain (MHC) is an important myofibrillar protein, which largely dictates the rate of force development and maximum shortening velocity of cross-bridge formation, thus forming the basis for the most accepted and widely used method of fibre type classification [22]. MHC-based fibre types are classified as type I, IIA, IID(X) and IIB that contain the corresponding MHC isoforms listed in increasing order of shortening velocity: MHCI, MHCIIa, MHCIId(x) and MHCIIb [22]. Chronic low-frequency stimulation (CLFS) is a model of endurance exercise training that induces fast-to-slow fibre type transformations that follow the “next nearest-neighbour” rule (as reviewed in [21, 23]). According to this rule, hybrid fibre types,

which co-express MHC-isoforms within a single fibre, bridge the gaps between the pure fibre types undergoing a predictable pattern of fast-to-slow transformation as follows: IIB  $\rightarrow$  IID(X)/B  $\rightarrow$  IID(X)  $\rightarrow$  IIA/D(X)  $\rightarrow$  IIA  $\rightarrow$  I/IIA  $\rightarrow$  I. Additionally, CLFS-induced fast-to-slow fibre type transformations occur in the absence of fibre injury in the rat and are associated with increases in satellite cell content, activity and fusion to transforming fibres [7, 17, 25, 26, 28].

Satellite cells are myogenic stem cells associated with adult skeletal muscle fibres that underlie the regenerative, and possibly adaptive, potential of muscle. It is well established that, in response to skeletal muscle hypertrophic stimuli or damage, quiescent satellite cells begin to actively cycle and fuse with existing myofibres or with each other, creating new myonuclei or forming new myofibres, respectively (as reviewed by [1, 5, 12, 20, 36]). As Schultz and Darr [35] and Bamman [4] point out, however, the role of satellite cells in endurance exercise-induced skeletal muscle fast-to-slow fibre type adaptation in the absence of injury is less clear. Recently, we showed that, in the absence of a viable satellite cell population in rat tibialis anterior muscles, long-term (21 days) CLFS-induced fast-to-slow fibre type transformations within the fast fibre population occurred normally [17]. The final transformation, however, from fast type IIA to slow type I fibres was prevented [17]. At this time point, 80–90% of fast-to-slow fibre type transformations have already occurred [13], suggesting the primary roles of satellite cells during long-term CLFS-induced fast-to-slow fibre type transformations are to (1) maintain stability of the transformed state [35] within the fast fibre types and (2) allow the final fast-twitch to slow-twitch adaptation [17].

On the other hand, short-term CLFS-induced fast-to-slow fibre type transformations are known to go through a unique period of rapid transformation within the first 10 days. Jaschinski et al. [13] detected fast-to-slow MHC isoform transformations beginning at the mRNA level after 3 days of CLFS that rapidly continued to change through 10 days. Corresponding changes at the MHC protein level first occurred at 5 days of stimulation and were found to be most rapidly transforming by 10 days of CLFS [13, 25, 26]. Interestingly, maximum satellite cell activity and fusion to transforming fibres, mostly within the fast fibre population, have also been shown to occur between 5 and 10 days of CLFS [25, 26]. Collectively, these observations suggest satellite cells may play an active role in the early phase of adaptation to CLFS, especially within the fast fibre population.

The purpose of the present study was to therefore test the hypothesis that, in the absence of a viable satellite cell population, short-term CLFS-induced fast-to-slow fibre type transformations would be (1) attenuated in the fast fibre population and (2) prevented in the final fast-twitch to slow-twitch adaptation. CLFS-induced satellite cell activa-

tion has not been investigated before 5 days in vivo. In light of the rapid CLFS-induced fast-to-slow transformations seen at the MHC mRNA and protein levels, it seems plausible that substantial satellite cell activation may occur within the first 4 days. CLFS was therefore applied for 1 to 10 days. In order to sustain a nonviable satellite cell population throughout this time, tibialis anterior muscles were exposed to a 25-Gy dose of  $\gamma$ -irradiation before the onset of CLFS and at regular intervals throughout the stimulation period [17]. Satellite cell proliferation was assessed by continuous labelling with 5-bromo-2'-deoxyuridine (BrdU) in vivo, followed by immunolocalisation [34]. MHC-based fibre type transformations were evaluated at the mRNA level by real-time reverse transcriptase-polymerase chain reaction (RT-PCR) [39] and at the protein level by sodium dodecyl sulfate polyacrylamide gel electrophoresis [11, 24] and immunohistochemistry [27, 28].

## Methods

**Animal treatment and care** Fifty-four adult male Wistar rats (Charles River Laboratories, Montreal, PQ, Canada) weighing  $320 \pm 3$  g (mean  $\pm$  SEM) were used in this study. Animals were individually housed under controlled environmental conditions (22°C with alternating 12 h light and dark cycles) and received standard rat chow and water ad libitum. All animal procedures were carried out in accordance with the guidelines of the Canadian Council for Animal Care (CCAC) and received ethical approval from the University of Alberta. Animals were randomly assigned to one of the following nine groups receiving: sham operation of the left leg only (Control);  $\gamma$ -irradiation plus 1 day (1d IRR-Stim), 2 days (2d IRR-Stim), 5 days (5d IRR-Stim) or 10 days (10d IRR-Stim) of CLFS of the left leg only; 1 day (1d Stim), 2 days (2d Stim), 5 days (5d Stim) or 10 days (10d Stim) of CLFS only ( $n=6$ , animals each group).

It has been previously shown that low doses of  $\gamma$ -irradiation alone (i.e. a single 60 Gy dose or three weekly 25 Gy doses) do not cause skeletal muscle fibre damage [14] or MHC protein, mRNA expression and metabolic abnormalities [17]. In accordance with the guidelines of the CCAC, a Control plus  $\gamma$ -irradiation group could not be justified as ethical and was therefore not included in this study. Unstimulated contralateral right legs served as internal controls. The application of CLFS, however, elicited a compensatory effect in the contralateral control muscles due to increased weight bearing, as previously observed [17, 26, 28], therefore comparisons were made to Control.

**Chronic low-frequency stimulation and BrdU labelling** CLFS (10 Hz, impulse width 380  $\mu$ s, 12 h day<sup>-1</sup>) was applied

across the left common peroneal nerve, directed to the tibialis anterior muscle for one, two, five or ten consecutive days [24, 37]. Animals received a continuous infusion of BrdU ( $10 \text{ mg ml}^{-1}$ ) via subcutaneously implanted Alzet® mini-osmotic pumps (model 2ML1,  $10 \mu\text{l h}^{-1}$  release rate and 2 ml volume) [34], which were replaced 1 week later in those animals receiving 10 days of stimulation.

**Gamma-irradiation** One day before the onset of stimulation, satellite cells of the left tibialis anterior muscle were sterilised as before [17]. Briefly, anaesthetised animals [ $75 \text{ mg (kg body weight)}^{-1}$  ketamine,  $10 \text{ mg (kg body weight)}^{-1}$  xylezene and  $0.5 \text{ mg (kg body weight)}^{-1}$  acepromazine maleate] were placed in a Gammacell 40 cesium-137 irradiation unit (Health Services Laboratory Animal Services, University of Alberta), and the left anterior crural compartment was exposed to a 25-Gy dose of  $\gamma$ -irradiation ( $0.56 \text{ Gy min}^{-1}$ ), while the remainder of the animal was shielded by two 2.5 cm thick lead plates. 10d IRR-Stim received a second 25 Gy dose of  $\gamma$ -irradiation 1 week later.

**Muscle sampling** Upon completion of the stimulation period, animals were anaesthetised, and the tibialis anterior muscles were excised from both hindlimbs, quickly fixed in a slightly stretched position and frozen in melting isopentane ( $-159^\circ\text{C}$ ). Muscles were stored in liquid nitrogen ( $-196^\circ\text{C}$ ). Animals were then killed with an overdose of Euthanyl [ $100 \text{ mg (kg body weight)}^{-1}$ ; Bimedia-MTC Animal Health Inc., Cambridge, ON, Canada] followed by exsanguination.

**Antibodies** The following monoclonal antibodies directed against adult and embryonic MHC isoforms [32, 33] were harvested from hybridoma cell lines obtained from the American Type Culture Collection (Manassas, VA, USA): BA-D5 (IgG, anti-MHCI), SC-71 (IgG, anti-MHCIIa), BF-F3 (IgM, anti-MHCIIb) and BF-45 (IgG, anti-MHC-embryonic). Clone BF-35 (purified IgG, not MHCIIx; also known as MHCIIId) was a generous gift from Prof. S. Schiaffino, Padova, Italy). Mouse monoclonal anti-BrdU (clone BMC 9318) was obtained from Roche Diagnostics Corporation (Indianapolis, IN, USA). Biotinylated horse anti-mouse IgG (rat-absorbed, affinity-purified) and biotinylated goat anti-mouse IgM were obtained from Vector Laboratories, Inc. (Burlingame, CA, USA).

**Immunohistochemistry for myosin and BrdU** Ten-micrometre-thick transverse frozen sections were collected from the mid-belly of each tibialis anterior muscle. Immunostaining was completed according to established protocols for MHC isoforms [27, 28] and BrdU [34]. Briefly, sections were fixed for 15 min in 70% (v/v) ethanol, washed once in

phosphate-buffered saline (PBS) with 0.1% (v/v) Tween-20 (PBS-T), twice with PBS and then incubated for 15 min in 3% (v/v)  $\text{H}_2\text{O}_2$  in methanol. Sections stained for BrdU were then incubated for 1 h in 2 N HCl and washed as before. Sections stained for BA-D5, SC-71, BF-35, BF-45 and BrdU were incubated for 1 h in a blocking solution [BS-1: 1% (w/v) bovine serum albumin and 10% (v/v) horse serum in PBS-T, pH 7.4] containing avidin-D blocking reagent (Vector Laboratories). Sections stained for BF-F3 were incubated in a similar blocking solution, with the exception that goat serum was substituted for horse serum (BS-2). Sections were incubated overnight at  $4^\circ\text{C}$  with a primary antibody that was diluted in its corresponding blocking solution containing biotin blocking reagent (Vector Laboratories). Biotinylated horse anti-mouse IgG (BA-D5; SC-71; BF-35; BF-45; anti-BrdU) or biotinylated goat anti-mouse IgM (BF-F3) was then applied for 1 h (Vector Laboratories). After several washings, sections were incubated with Vectastain ABC Reagent according to the manufacturer's instructions (Vector Laboratories) and reacted with 0.07% (w/v) diaminobenzidine, 0.05% (v/v)  $\text{H}_2\text{O}_2$  and 0.03% (w/v)  $\text{NiCl}_2$  in 50 mM Tris-HCl (pH 7.5). All sections were subsequently dehydrated, cleared and mounted in Entellan (Merck, Darmstadt, Germany).

**Immunohistochemical analyses** MHC isoform semi-quantitative analyses were completed with a Leitz Diaplan microscope (Ernst Leitz Wetzlar GmbH, Germany) fitted with a Pro-Series High Performance Charge-Coupled Digital camera (Cohu, San Diego, CA, USA), Image-Pro Plus imaging software (Media Cybernetics, Bethesda, MD, USA) and a custom-designed analytical program [26]. A similar number of fibres, totalling 60,996, were examined from each group for the various MHC isoforms from three representative cross-sectional areas of tibialis anterior muscles (i.e. deep, middle and superficial regions). Type I, IIA, IIB and embryonic fibres were identified by positive staining, and type IID(X) fibres were identified by the absence of staining with all antibodies directed against the various MHC isoforms. BrdU semi-quantitative analysis was completed with a Leka DMRBE microscope (Leica Microsystems GmbH Wetzlar, Germany) at  $\times 640$  magnification. BrdU-positive nuclei were enumerated on cross-sections of all tibialis anterior muscles. A total area of  $4.4 \pm 0.06 \text{ mm}^2$  was examined for each muscle.

**Electrophoretic analysis of MHC protein isoforms** Quantitative MHC isoform analyses were completed as previously described [11, 24]. Briefly, frozen tibialis anterior muscles were homogenised in an ice cold buffer containing 100 mM  $\text{NaP}_2\text{O}_7$  (pH 8.5), 5 mM EGTA, 5 mM  $\text{MgCl}_2$ , 0.3 mM KCl, 10 mM dithiothreitol (Sigma-Aldrich, Oakville, ON, Canada) and  $5 \text{ mg ml}^{-1}$  of a protease inhibitor cocktail

**Table 1** Rat specific real-time reverse-transcriptase polymerase chain reaction primers and probes

Target	Forward Primer	Reverse Primer	Probe
MHCI $\beta$	5'-GCAGTTGGATGAGCGACTCA-3'	5'-TCCTCAATCTGGCGTTGA-3'	5'-AGAAGGACTTTGAGTTAAAT-3'
MHCIIa	5'-GGCGGCAAGAAGCAGATC-3'	5'-TTCCGTTCTGCTCACTCTCT-3'	5'-AGGCCAGAGTGCCTG-3'
MHCII d(x)	5'-GGCGGCAAGAAGCAGATC-3'	5'-TTCGTTTTCAACTTCTCCTTCAAGT-3'	5'-AGGCCAGGGTCCG-3'
MHCIIb	5'-GGCGGCAAGAAGCAGATC-3'	5'-TTTTCCACCTCGTTTTCAAGCT-3'	5'-TGGAGGCCAGAGTGA-3'

(Complete, Roche Diagnostics). The supernatants of centrifuged samples were diluted 1:1 with glycerol and stored at  $-20^{\circ}\text{C}$  until analysed. Extracts were diluted in modified Laemmli lysis buffer to a concentration of  $0.2\ \mu\text{g}\ \mu\text{l}^{-1}$ , boiled for 6 min and cooled on ice prior to gel loading. MHC isoforms were separated electrophoretically on 7% polyacrylamide gels containing glycerol, under denaturing

conditions. Samples ( $1\ \mu\text{g}$  total protein per lane) were electrophoresed in duplicate at 275 V for 24 h at  $8^{\circ}\text{C}$ . Gels were then fixed and MHC isoforms were detected by silver staining and evaluated by integrated densitometry (ChemGenius, GeneSnap and GeneTools, Syngene, UK).

**MHC mRNA analyses by real-time RT-PCR** Patterns of MHC isoform expression were further analysed at the mRNA level using real-time RT-PCR. RNA extraction was performed according to an established procedure [39]. The concentrations and purity of RNA extracts were evaluated by measuring the absorbance at 260 and 280 nm, respectively, using a NanoDrop ND 1000 system (Rose Scientific, Edmonton, AB, Canada). cDNA synthesis was performed according to an established procedure [3]. Briefly, random oligo (dT<sub>15</sub>) primers (Invitrogen, Life Technologies, Burlington, ON, Canada) and Moloney murine leukemia virus DNA polymerase (Invitrogen, Life Technologies) were added to diluted samples ( $1\ \mu\text{g}\ \mu\text{l}^{-1}$ ), and reverse transcription was performed for 1 h at  $37^{\circ}\text{C}$ . Primers (Invitrogen, Life Technologies) and Taqman-MGB probes (Applied Biosystems, Foster City, CA, USA) were designed with European Molecular Biology Laboratory-European Bioinformatics Institute and aligned using Clustal W for rat MHCII $\beta$  (X15939), MHCIIa (L13606), MHCII d(x) (XM 213345) and MHCIIb (L24897) (Table 1). Real-time PCR was performed on  $1\ \mu\text{l}$  cDNA samples, in duplicate, using an ABI 7900HT thermocycler (Applied Biosystems). 18S RNA (Applied Biosystems) was used as the endogenous control. Relative changes in MHC isoform gene expression were determined using the  $2^{-\Delta\Delta\text{Ct}}$  method of analysis [16]. Inter-assay variation was evaluated by repeated analysis of a known sample on each 96-well plate and confirmed to be negligible. Additionally, the amplification efficiencies of the MHC isoforms and 18S were similar.

**Statistical analyses** Data are summarised as means $\pm$ SEM. Within each group (i.e. Stim or IRR-Stim) differences were assessed compared to Control (e.g. 1d, 2d, 5d or 10d Stim versus Control) using a one-way analysis of variance (ANOVA). Differences between the IRR-Stim and Stim groups at each time point were assessed using a two-way ANOVA. When a significant *F* ratio was found, differences were located using the Newman–Keuls post hoc analysis.

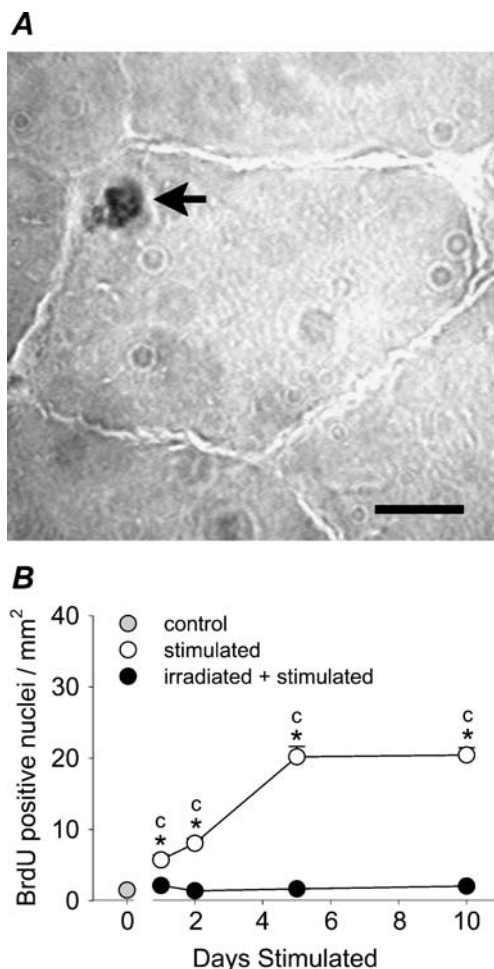


**Fig. 1** **a** Photomicrograph of representative immunohistochemical BrdU stain used to identify proliferating and previously proliferating satellite cells (arrow) in rat tibialis anterior muscles. Bar represents  $10\ \mu\text{m}$ . **b** Number of proliferating and previously proliferating satellite cells per unit area in rat tibialis anterior muscles. Statistical symbols indicate: <sup>c</sup> difference from Control, asterisk difference between Stim and IRR-Stim of the same number of days of stimulation ( $P < 0.05$ )

Differences were considered significant at  $P < 0.05$ . There were no differences between the left and right legs of Control, as determined by the  $t$  test for dependent samples; therefore these data were pooled.

## Results

**Animal and muscle weights** All animals initially weighed  $321 \pm 3$  g and similarly gained  $26 \pm 5$  g during 10 days of stimulation. Additionally, animal weights did not differ between Stim and IRR-Stim groups of the same number of days of stimulation at all other time points (i.e. 1d, 2d and 5d). Tibialis anterior muscle weights were not different between the left and right legs of all groups.

**Satellite cell activity** An established method was used to assess satellite cell proliferation [17]. The number of proliferating and previously proliferating satellite cells was determined by quantifying BrdU staining. Only those stained nuclei that were unambiguously fused to existing muscle fibres were counted, as shown in Fig. 1a. CLFS first induced an increase in BrdU-positive nuclei at 1 day of stimulation (i.e. 1d Stim; 3.9-fold increase) up to a maximum of a 13.8-fold increase at 10 days of stimulation (i.e. 10d Stim) compared with Control (Fig. 1b). In contrast,  $\gamma$ -irradiation plus 1 day (i.e. 1d IRR-Stim;  $2.1 \pm 0.3$  positively stained nuclei  $\text{mm}^{-2}$ ), 2 days (i.e. 2d IRR-Stim;  $1.4 \pm 0.2$ ), 5 days (i.e. 5d IRR-Stim;  $1.6 \pm 0.1$ ) or 10 days

(i.e. 10d IRR-Stim;  $2.0 \pm 0.3$ ) of stimulation did not alter the number of proliferating and previously proliferating satellite cells compared with Control (Fig. 1b;  $1.5 \pm 0.2$ ).

**MHC mRNA expression** CLFS-induced MHC-isoform transformations at the mRNA level occurred in the direction of fast-to-slow at 10 days of stimulation [i.e. 10d Stim; MHCIIb mRNA  $\rightarrow$  MHCIIId(x) mRNA  $\rightarrow$  MHCIIa mRNA  $\rightarrow$  MHCI mRNA]. Specifically, 10d Stim MHCI mRNA (Fig. 2a), MHCIIa mRNA (Fig. 2b) and MHCIIId(x) mRNA (Fig. 2c) increased compared with Control, with no increase in the expression of MHCIIb mRNA (Fig. 2d). In 10d IRR-Stim, increases in MHC mRNA levels were observed in 10d IRR-Stim for MHCI (Fig. 2a) and MHCIIa (Fig. 2b) compared with Control. Importantly, however, Stim MHCI mRNA was 4.8-fold larger compared with IRR-Stim, which showed a trend towards significance (Fig. 2a; main effect  $P = 0.067$ ). Additionally, 10d Stim MHCIIId(x) mRNA was 6.9-fold greater compared with 10d IRR-Stim (Fig. 2c).

**MHC-isoform transformations** A representative gel showing the quantitative analytical method used to measure MHC-isoform protein content in muscle extracts is illustrated in Fig. 3a. CLFS-induced fast-to-slow MHC-isoform transformations were first observed at 5 days of stimulation [i.e. 5d Stim; MHCIIb  $\rightarrow$  MHCIIId(x)  $\rightarrow$  MHCIIa] and continued further at 10 days of stimulation [i.e. 10d Stim; MHCIIb  $\rightarrow$  MHCIIId(x)  $\rightarrow$  MHCIIa  $\rightarrow$  MHCI] (Fig. 3b). Specifically, the slower MHCI and MHCIIa content of 10d Stim both increased 1.9-fold with a concomitant 1.3-fold

**Fig. 2** Fold changes in MHCI mRNA (a), MHCIIa mRNA (b), MHCIIId(x) mRNA (c) and MHCIIb mRNA (d) gene expression levels in rat tibialis anterior muscles. Statistical symbols indicate: <sup>c</sup> difference from Control, \* difference between Stim and IRR-Stim of the same number of days of stimulation ( $P < 0.05$ )

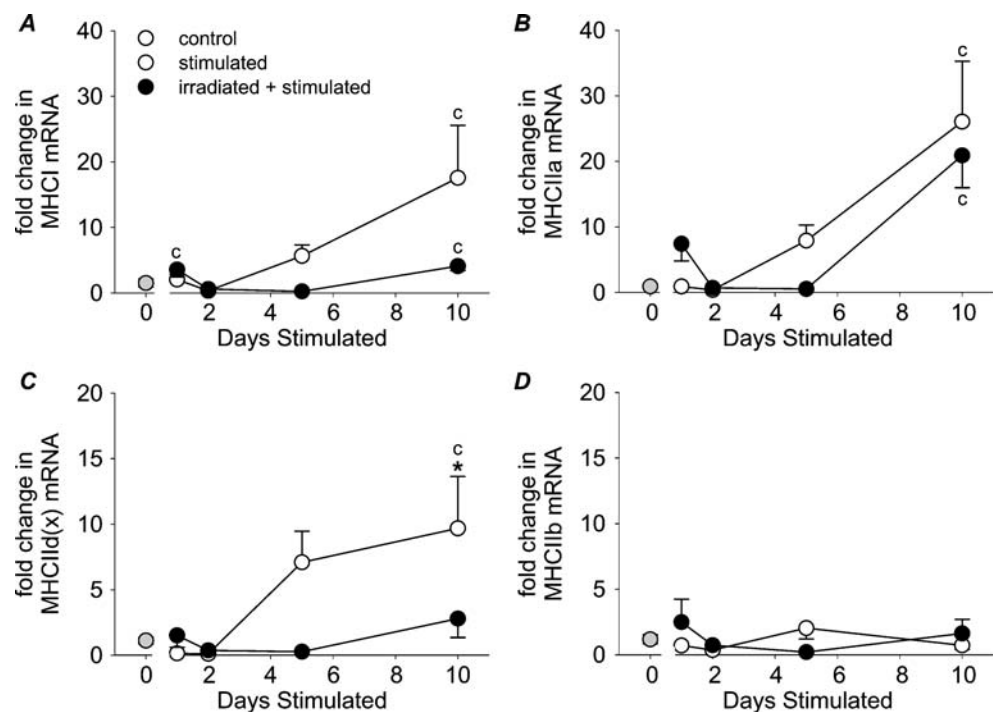
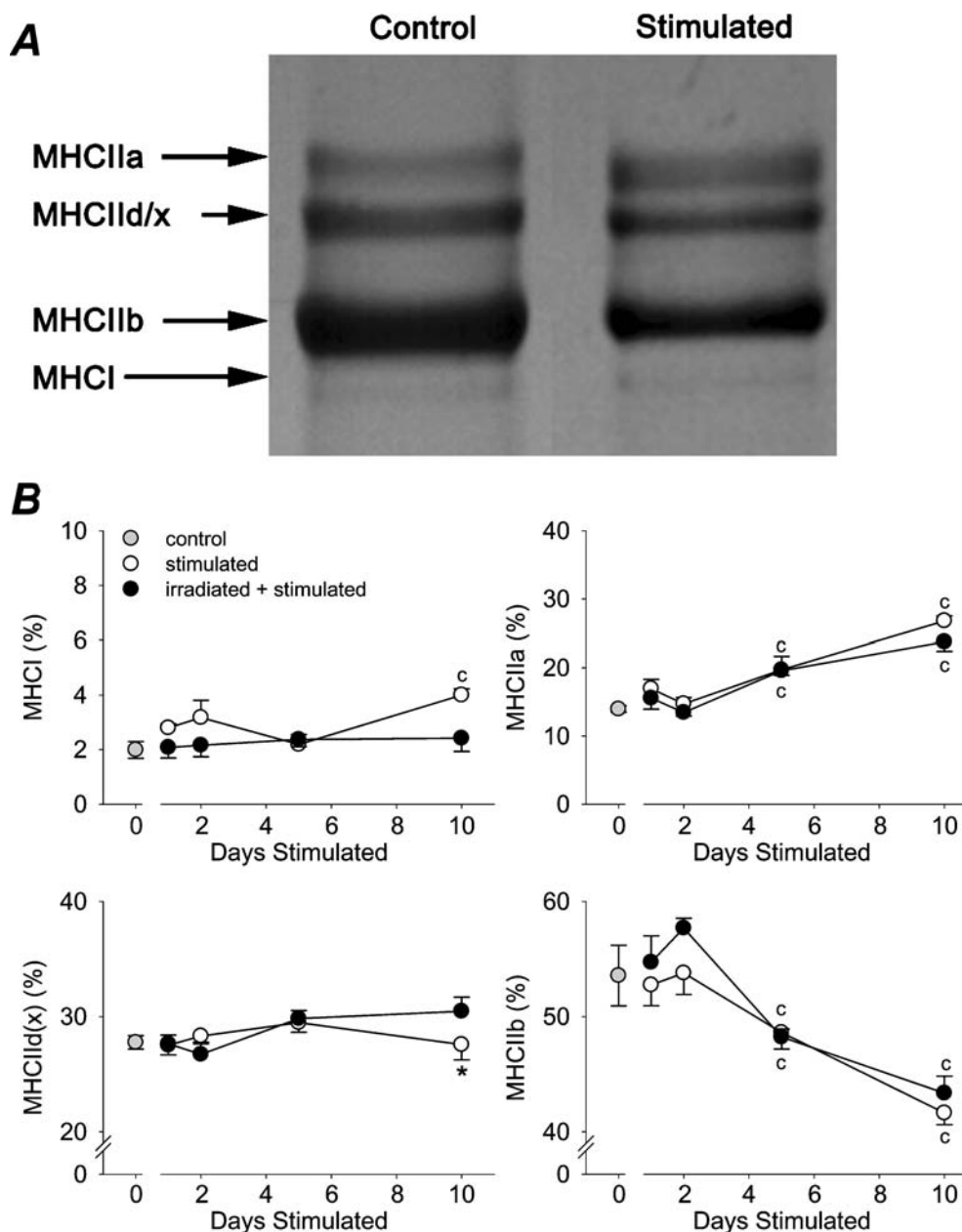


**Fig. 3 a** Example of the electrophoretic method used to quantify MHC isoform composition of rat tibialis anterior muscles. Control and stimulated (10d Stim) are shown. **b** Percentage of MHCI, MHCIIa, MHCIIc(x) and MHCIIb distribution in rat tibialis anterior muscles as determined by densitometric evaluation of duplicate gels. Statistical symbols indicate: *c* difference from Control, *asterisk* difference between Stim and IRR-Stim of the same number of days of stimulation ( $P < 0.05$ )



decrease in MHCIIb content compared with Control. 10d IRR-Stim MHC fast-to-slow transformations only occurred amongst the fast MHC isoforms as shown by a 1.7-fold increase in MHCIIa along with a 1.3-fold decrease in MHCIIb content. Importantly, the relative content of IRR-Stim MHCI was not different from Control, and the main effect of MHCII content was significantly greater in Stim compared with IRR-Stim ( $P < 0.02$ ). This finding is consistent with our previous observations that, with satellite cell ablation, the final fast MHCIIa to slow MHCI transformation does not occur [17]. Interestingly, the relative content of MHCIIc(x) in 10d IRR-Stim was significantly larger than in 10d Stim. This, however, likely reflects the

restriction of fast-to-slow transformations to the fast MHC isoforms following satellite cell ablation.

*Fibre type transformations* Detailed fibre type analysis, which included the detection of all pure and hybrid fibre types, were assessed by semi-quantitative immunohistochemical analyses on serial sections (Fig. 4) in the deep, middle and superficial regions of each tibialis anterior muscle. CLFS-induced fast-to-slow fibre type transformations were, however, only observed in the deep and middle regions, and therefore, our analysis was restricted to these areas. As similarly observed in MHC-isoform proportions, fast-to-slow fibre type transformations began at 5 days of

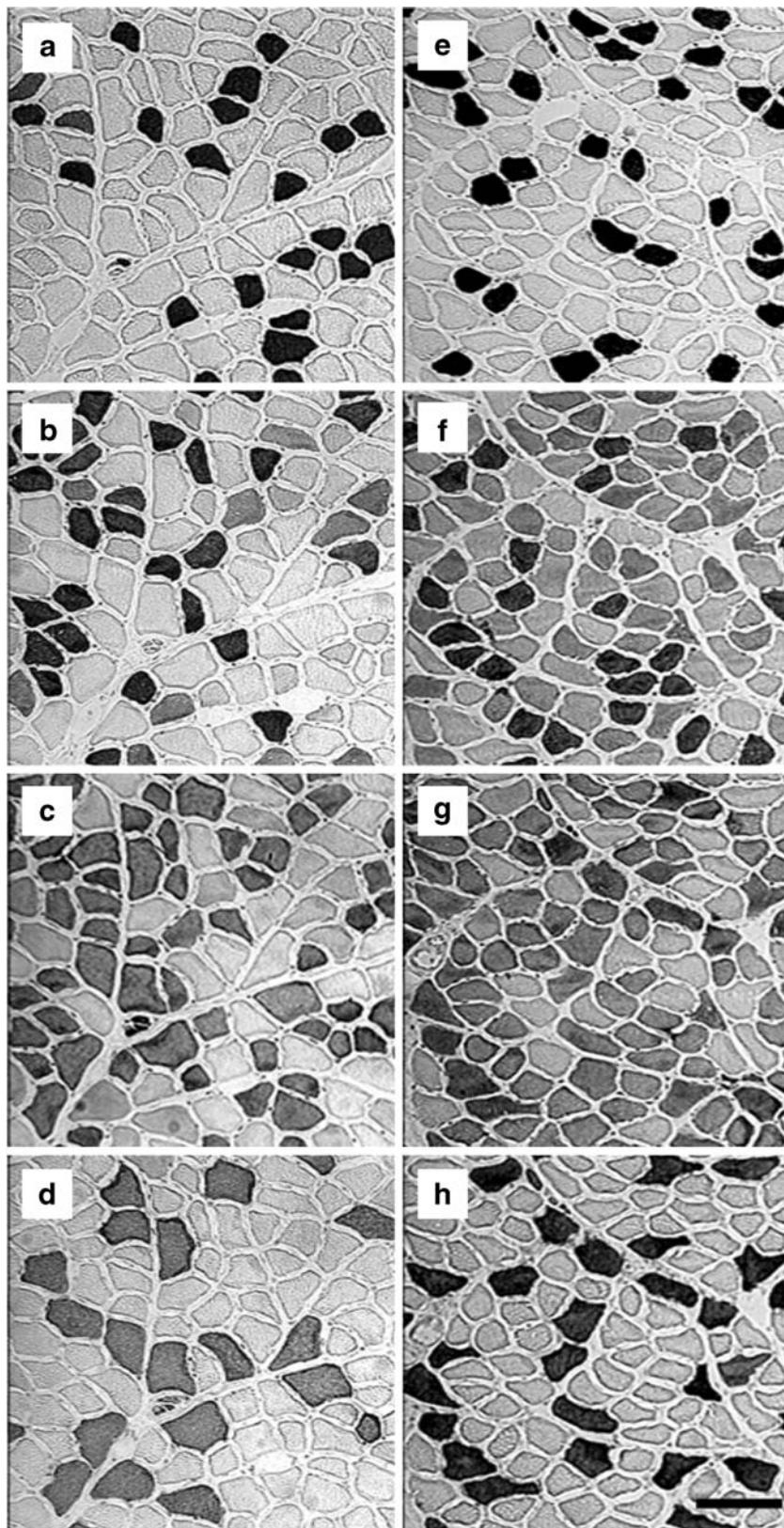
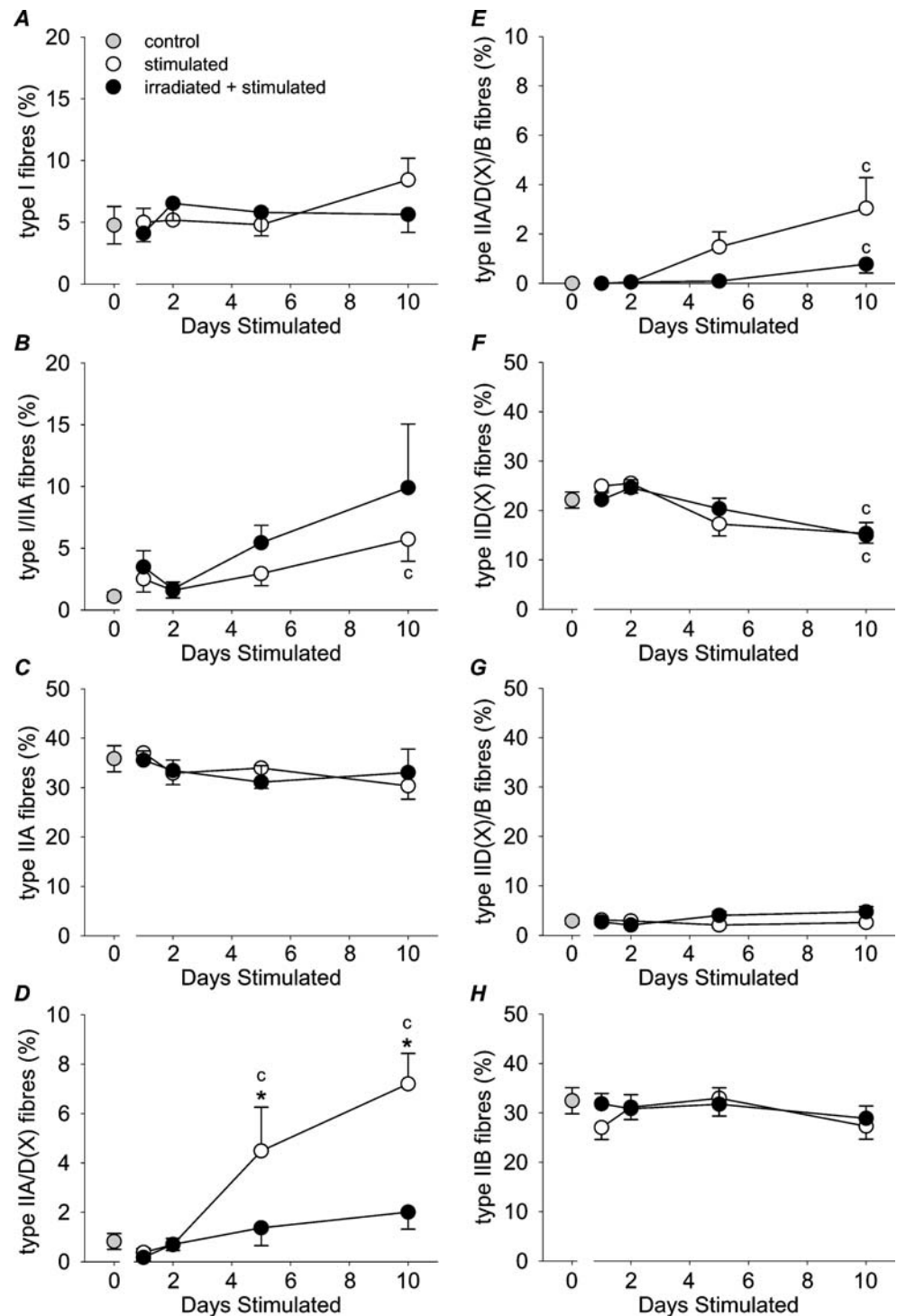


**Fig. 4** Representative photomicrographs of MHC isoform immunohistochemistry of Control (**a–d**) and 10 day stimulated rat tibialis anterior muscles (**e–h**). **a, e** Immunostains for MHC I (clone BA-D5);

**b, f** immunostains for MHC IIa (clone SC-71); **c, g** immunostains for all MHCs except MHC II d(x) (clone BF-35); **d, h** immunostains for MHC II b (clone BF-F3). *Bar* represents 100  $\mu$ m

**Fig. 5** The proportion of pure and hybrid fibre types I (a), I/IIA (b), IIA (c), IIA/D(X) (d), IIA/D(X)/B (e), IID(X) (f), IID(X)/B (g) and IIB (h) in rat tibialis anterior muscles. Fibre types are listed in order from slowest (i.e. type I) to fastest (i.e. type IIB). Statistical symbols indicate: <sup>c</sup> difference from Control, <sup>\*</sup> difference between Stim and IRR-Stim of the same number of days of stimulation ( $P < 0.05$ )



stimulation [i.e. IID(X) → IIA] and further continued at 10 days of stimulation [i.e. IID(X) → IIA → I] (Fig. 5). Specifically, 10d Stim displayed increases in the proportions of the slower type I/IIA (Fig. 5b), IIA/D(X) (Fig. 5d) and IIA/D(X)/B (Fig. 5e) fibres with a concomitant decrease in the proportion of the faster type IID(X) fibres (Fig. 5f) compared with Control. At 10 days of stimulation in IRR-Stim (i.e. 10d IRR-Stim), however, these fast-to-

slow fibre type transformations were limited to the fast fibre population. Specifically, 10d IRR-Stim only displayed increases in the proportions of the hybrid type IIA/D(X)/B fibres (Fig. 5e) with a concomitant decrease in the proportion of the pure type IID(X) fibres (Fig. 5f) compared with Control. Most importantly, the emergence of hybrid fibre types that are a hallmark of the response to CLFS (reviewed in [21]) was not the same in 10d Stim and IRR-



Stim. Specifically, the proportion of type IIA/D(X) fibres in 10d IRR-Stim was significantly lower compared with 10d Stim (Fig. 5d). The proportion of type IIA/D(X)/B fibres was also significantly lower in IRR-Stim compared with Stim (Fig. 5e; main effect  $P < 0.02$ ). Additionally, consistent with our previous findings [20], proportions of the slowest type I (Fig. 4a) and type I/IIA (Fig. 4b) fibres in all IRR-Stim groups were not different from Control. Embryonic MHC was not detected in extrafusal fibres.

## Discussion

The findings of the present study extend our previous works [17, 25, 26, 28] by investigating early time points (i.e. 1 to 10 days) of CLFS-induced fast-to-slow fibre type transformations when maximum satellite cell activity and fusion to rapidly transforming fibres are known to occur, especially within the fast IIB and IID(X) fibre populations [25, 26]. In the current study, the absence of increases in BrdU-positive nuclei in all IRR-Stim groups clearly shows that satellite cell proliferation was ablated throughout the entire study, thus allowing us to investigate the early adaptive phase of CLFS-induced fast-to-slow fibre type transformations in the absence of a viable satellite cell population. The novel findings of this study are that (1) CLFS-induced satellite cell proliferation *in vivo* begins at 1 day of stimulation and continues throughout the 10-day stimulation period; in the absence of a viable satellite cell population, fast-to-slow fibre type transformations during short-term CLFS are (2) attenuated in the fast fibre population and (3) prevented from the final fast-twitch to slow-twitch adaptation.

### CLFS model of muscle training

CLFS is a model of endurance muscle training resulting in skeletal muscle fast-to-slow fibre type transformations and associated fibre atrophy, which is ideal for studying the effects of increased contractile activity on various skeletal muscle structural, functional, metabolic and molecular properties in the absence of fibre damage in rat (as reviewed by [21, 23]). The CLFS-induced decrease in fibre cross-sectional area, specifically in the fast IIB and IID(X) fibre types, is the result of transformation to a slower fibre type, as opposed to fibre degeneration [7, 17]. CLFS induces rapid and predictable fast-to-slow fibre type transformations by mimicking the electrical discharge pattern of slow motoneurons that innervate slow-twitch muscles. Unlike other rodent exercise models such as voluntary wheel running, however, it causes synchronous recruitment of all targeted motor units, including those not normally

recruited during endurance exercise training [23]. In doing so, the adaptive potential of CLFS-targeted muscles is maximally challenged. Also, the standardised and highly reproducible conditions of CLFS allows for activity-induced fast-to-slow phenotypic changes to occur in a well-defined time-dependent manner [13, 21]. For these reasons, the CLFS model of muscle training was used in the present study.

### Fibre type transformations in irradiated muscles

There are a limited number of studies that have investigated exercise-induced fast-to-slow fibre type transformations in muscles that have also been exposed to ionising radiation [2, 15, 17, 29, 30]. Results from our laboratory are in contrast with those studies which reported no attenuation of fast-to-slow fibre type transformations in response to overload [2, 29, 30] or voluntary wheel running [15] in muscles that were also exposed to ionising radiation. The major differences between those studies [2, 15, 29, 30] and ours were three-fold. First, disruption of satellite cell mitotic activity after a single 25 Gy dose of  $\gamma$ -irradiation has been shown to occur for only 7 days [19] with significant recovery taking place 9 and 12 days post-irradiation [18, 19, 40]. We therefore administered weekly 25 Gy doses of  $\gamma$ -irradiation to ensure continuous mitotic disruption of the satellite cell pool, while previous studies [2, 15, 29, 30] only administered a single 25-Gy dose of ionising radiation before the onset of exercise. Consequently, in those studies, a significant amount of satellite cell proliferation was observed in response to 14 days of voluntary wheel running in mouse plantaris muscles [15], and a greater skeletal muscle DNA content was reported after 15 days of compensatory overload in rat plantaris muscles [2]. Second, in order to determine the specific effectiveness of ionising radiation on preventing satellite cell proliferation and subsequent myonuclei contribution, only Li et al. [15] and our studies directly measured proliferating and previously proliferating satellite cells *in vivo*. On the other hand, Adams et al. [2] measured DNA content and Rosenblatt and Parry [30] reported myonuclear-to-myoplasmic volume ratio or assumed satellite cell sterilisation [29]. Third, comprehensive and detailed MHC isoform identification methods (i.e. immunohistochemistry, gel electrophoresis and RT-PCR) that detect both pure and hybrid fibre types were used in our studies to assess fast-to-slow fibre type transformations, whereas others have only quantified the proportions of MHC protein isoforms [2, 15] or restricted their analyses to only adult pure fibre types [29, 30]. Taken together, these differences likely accounted for our ability to detect attenuation of fast-to-slow fibre type transformations in the IRR-Stim muscles.

## Fast-to-slow fibre type transformations and myonuclear domain

Schultz and Darr [35] were first to introduce the idea of satellite cell involvement in fast-to-slow fibre type transformations. They hypothesised that since slow-twitch skeletal muscle fibres contain a larger number of myonuclei, smaller cross-sectional areas and cytoplasmic volume [8, 9] and therefore, smaller myonuclear domain sizes compared with fast-twitch fibres [6, 31, 35, 38], satellite cells play an obligatory role in maintaining the newly fast-to-slow transformed state. Smaller myonuclear domains are presumably a requirement for higher biosynthetic activities in slow-twitch fibres [10]. For example, the transformation from a fast-twitch to a slower-twitch fibre type would include a decrease in myonuclear domain size by the addition of new myonuclei coupled with a decrease in fibre cross-sectional area and cytoplasmic volume. The results of our previous studies [17, 26] support this hypothesis, while the data of our current study further indicates that satellite cells also facilitate fast-to-slow fibre type transformations during the early phase of adaptation to CLFS.

We have previously shown that, during short-term CLFS, maximal satellite cell activity and fusion were primarily targeted to the fast IIB and IID(X) fibre types, which preceded fast-to-slow fibre type transformations [13, 25, 26] and preceded decreases in the cross-sectional areas of those fibre types [7]. Therefore, the myonuclear domain sizes of the fast fibre types, which are actively undergoing fast-to-slow transformations, are first to decrease by the incorporation of satellite cells during short-term CLFS. By comparison during long-term CLFS, further reductions in myonuclear domain sizes occur via decreases in fibre cross-sectional area of the newly transformed fibres and to a lesser extent by the fusion of satellite cell progeny [17]. In the absence of a viable satellite cell population, results from the current study show that short-term CLFS-induced fast-to-slow fibre type transformations, within the fast fibre population, were attenuated. These findings indicate that satellite cell activity is important during short-term CLFS to reduce the myonuclear domain sizes of the fast fibre types, thus increasing necessary biosynthetic activity, allowing them to transform without delay. In contrast, satellite cells appear to play an obligatory role in the final transformation from fast type IIA to slow type I fibres (present study; [17]).

## Conclusions

Results of the present study show that, in the absence of a viable satellite cell population within rat tibialis anterior muscles, short-term CLFS-induced fast-to-slow fibre type transformations are attenuated in the fast fibre population.

Thus satellite cells appear to play an active role early on in the time course during CLFS-induced fast-to-slow fibre type transformations. Considerable adaptive potential does, however, exist within myonuclei and their domains up to a certain threshold beyond which satellite cells are required, especially for the final transformation from type IIA to type I fibres.

**Acknowledgements** This study was funded by research grants from the Natural Sciences and Engineering Council of Canada (NSERC; to C.T. Putman), the Alberta Heritage Foundation for Medical Research (AHFMR; to C.T. Putman), the Alberta Agricultural Research Institute (to W.T. Dixon and G.R. Foxcroft) and the Canadian Institute for Health Research (to T. Gordon). K.J.B. Martins was supported by NSERC and AHFMR graduate scholarships. M. Gallo was supported by NSERC and Izaak Walton Killam Memorial scholarships. The authors thank Prof. S. Schiaffino (Padova, Italy) for generously providing monoclonal antibody clone BF-35 (purified IgG, not MHCIIx). The authors also thank M. Burgquest for technical assistance. T. Gordon is an AHFMR Senior Investigator, and C.T. Putman is an AHFMR Senior Scholar.

## References

- Adams GR (2006) Satellite cell proliferation and skeletal muscle hypertrophy. *Appl Physiol Nutr Metab* 31:782–790
- Adams GR, Caiozzo VJ, Haddad F, Baldwin KM (2002) Cellular and molecular responses to increased skeletal muscle loading after irradiation. *Am J Physiol Cell Physiol* 283:C1182–C1195
- Bamford JA, Lopaschuk GD, MacLean IM, Reinhart ML, Dixon WT, Putman CT (2003) Effects of chronic AICAR administration on metabolic and contractile phenotype in rat skeletal muscle. *Can J Physiol Pharmacol* 81:1072–1082
- Bamman MM (2007) Take two NSAIDs and call on your satellite cells in the morning. *J Appl Physiol* 103:415–416
- Charge SB, Rudnicki MA (2004) Cellular and molecular regulation of muscle regeneration. *Physiol Rev* 84:209–238
- Cheek DB (1985) The control of cell mass and replication. The DNA unit—a personal 20-year study. *Early Hum Dev* 12:211–239
- Delp MD, Pette D (1994) Morphological changes during fiber type transitions in low-frequency-stimulated rat fast-twitch muscle. *Cell Tissue Res* 277:363–371
- Gibson MC, Schultz E (1982) The distribution of satellite cells and their relationship to specific fiber types in soleus and extensor digitorum longus muscles. *Anat Rec* 202:329–337
- Gibson MC, Schultz E (1983) Age-related differences in absolute numbers of skeletal muscle satellite cells. *Muscle Nerve* 6:574–580
- Goldberg AL (1967) Protein synthesis in tonic and phasic skeletal muscles. *Nature* 216:1219–1220
- Hämäläinen N, Pette D (1996) Slow-to-fast transitions in myosin expression of rat soleus muscle by phasic high-frequency stimulation. *FEBS Lett* 399:220–222
- Hawke TJ, Garry DJ (2001) Myogenic satellite cells: physiology to molecular biology. *J Appl Physiol* 91:534–551
- Jaschinski F, Schuler MJ, Peuker H, Pette D (1998) Changes in myosin heavy chain mRNA and protein isoforms of rat muscle during forced contractile activity. *Am J Physiol Cell Physiol* 274: C365–C370
- Lewis RB (1954) Changes in striated muscle following single intense doses of X-rays. *Lab Invest* 3:48–55

15. Li P, Akimoto T, Zhang M, Williams RS, Yan Z (2006) Resident stem cells are not required for exercise-induced fiber-type switching and angiogenesis but are necessary for activity-dependent muscle growth. *Am J Physiol Cell Physiol* 290: C1461–C1468
16. Livak KJ, Schmittgen TD (2001) Analysis of relative gene expression data using real-time quantitative PCR and the 2(-Delta Delta C(T)) Method. *Methods* 25:402–408
17. Martins KJ, Gordon T, Pette D, Dixon WT, Foxcroft GR, MacLean IM, Putman CT (2006) Effect of satellite cell ablation on low-frequency-stimulated fast-to-slow fibre-type transitions in rat skeletal muscle. *J Physiol* 572:281–294
18. McGeachie JK, Grounds MD, Partridge TA, Morgan JE (1993) Age-related changes in replication of myogenic cells in mdx mice: quantitative autoradiographic studies. *J Neurol Sci* 119:169–179
19. Mozdziak PE, Schultz E, Cassens RG (1996) The effect of in vivo and in vitro irradiation (25 Gy) on the subsequent in vitro growth of satellite cells. *Cell Tissue Res* 283:203–208
20. O'Connor RS, Pavlath GK (2007) Point:Counterpoint: Satellite cell addition is/is not obligatory for skeletal muscle hypertrophy. *J Appl Physiol* 103:1099–1100
21. Pette D (2002) The adaptive potential of skeletal muscle fibers. *Can J Appl Physiol* 27:423–448
22. Pette D, Staron RS (1997) Mammalian skeletal muscle fiber type transitions. *Int Rev Cytol* 170:143–223
23. Pette D, Staron RS (2000) Myosin isoforms, muscle fiber types, and transitions. *Microsc Res Tech* 50:500–509
24. Putman CT, Dixon WT, Pearcey J, MacLean IM, Jendral MJ, Kiricsi M, Murdoch GK, Pette D (2004) Chronic low-frequency stimulation up-regulates uncoupling protein-3 in transforming rat fast-twitch skeletal muscle. *Am J Physiol Regul Integr Comp Physiol* 287:R1419–R1426
25. Putman CT, Düsterhöft S, Pette D (1999) Changes in satellite cell content and myosin isoforms in low-frequency-stimulated fast muscle of hypothyroid rat. *J Appl Physiol* 86:40–51
26. Putman CT, Düsterhöft S, Pette D (2000) Satellite cell proliferation in low-frequency stimulated fast muscle of hypothyroid rat. *Am J Physiol Cell Physiol* 279:C682–C690
27. Putman CT, Kiricsi M, Pearcey J, MacLean IM, Bamford JA, Murdoch GK, Dixon WT, Pette D (2003) AMPK activation increases UCP-3 expression and mitochondrial enzyme activities in rat muscle without fibre type transitions. *J Physiol (Lond)* 551.1:169–178
28. Putman CT, Sultan KR, Wassmer T, Bamford JA, Skorjanc D, Pette D (2001) Fiber-type transitions and satellite cell activation in low-frequency-stimulated muscles of young and aging rats. *J Gerontol A Biol Sci Med Sci* 56:B510–B519
29. Rosenblatt DJ, Parry DJ (1992) Gamma irradiation prevents compensatory hypertrophy of overloaded mouse extensor digitorum longous muscle. *J Appl Physiol* 73:2538–2543
30. Rosenblatt DJ, Parry DJ (1993) Adaptation of rat extensor digitorum longous muscle to gamma irradiation and overload. *Pflügers Arch* 423:255–264
31. Roy RR, Monke SR, Allen DL, Edgerton VR (1999) Modulation of myonuclear number in functionally overloaded and exercised rat plantaris fibers. *J Appl Physiol* 87:634–642
32. Schiaffino S, Gorza L, Pitton G, Saggin L, Ausoni S, Sartore S, Lomo T (1988) Embryonic and neonatal myosin heavy chain in denervated and paralyzed rat skeletal muscle. *Dev Biol* 127:1–11
33. Schiaffino S, Gorza L, Sartore S, Saggin L, Ausoni S, Vianello M, Gundersen K, Lomo T (1989) Three myosin heavy chain isoforms in type 2 skeletal muscle fibres. *J Muscle Res Cell Motil* 10:197–205
34. Schultz E (1996) Satellite cell proliferative compartments in growing skeletal muscles. *Dev Biol* 175:84–94
35. Schultz E, Darr KC (1990) The role of satellite cells in adaptive or induced fiber transformations. In: Pette D (ed) *The dynamic state of muscle fibers*. Walter de Gruyter, Berlin, pp 667–679
36. Schultz E, McCormick KM (1994) Skeletal muscle satellite cells. *Rev Physiol Biochem Pharmacol* 123:213–257
37. Simoneau J-A, Pette D (1988) Species-specific effects of chronic nerve stimulation upon tibialis anterior muscle in mouse, rat, guinea pig and rabbit. *Pflügers Arch* 412:86–92
38. Tseng BS, Kasper CE, Edgerton VR (1994) Cytoplasm-to-myonucleus ratios and succinate dehydrogenase activities in adult rat slow and fast muscle fibers. *Cell Tissue Res* 275:39–49
39. Vinsky MD, Murdoch GK, Dixon WT, Dyck MK, Foxcroft GR (2007) Altered epigenetic variance in surviving litters from nutritionally restricted lactating primiparous sows. *Reprod Fertil Dev* 19:430–435
40. Wakeford S, Watt DJ, Partridge TA (1991) X-irradiation improves mdx mouse muscle as a model of myofiber loss in DMD. *Muscle Nerve* 14:42–50